JACS
JOURNAL OF THE AMERICAN CHEMICAL SOCIETY

ARTICLE

pubs.acs.org/JACS

Effect of Stereogenic Centers on the Self-Sorting, Depolymerization, and Atropisomerization Kinetics of Porphyrin-Based Aggregates

Floris Helmich, Maarten M. J. Smulders, Cameron C. Lee, Albertus P. H. J. Schenning,* and E. W. Meijer*

Institute for Complex Molecular Systems, Laboratory of Macromolecular and Organic Chemistry, Eindhoven University of Technology, P.O. Box 513, 5600 MB Eindhoven, The Netherlands

Supporting Information

ABSTRACT: We present our results on the mixing of different porphyrin molecules in supramolecular assemblies. Herein, chiral amplification experiments reveal the subtle role of the structural (mis)match between these monomers. We show that according to the "sergeant-and-soldiers" principle, a chiral porphyrin "sergeant" efficiently mixes with achiral "soldiers" in the same helical aggregate and strongly biases its handedness. However, when we mix two porphyrin enantiomers in a majority-rules experiment, no chiral amplification is observed at all, which is due to their narcissistic self-sorting into conglomerate-like aggregates. The mixing between two enantiomers in the same stack only occurs in a diluted-majority-rules experiment, in which enantiomeric mixtures of sergeants are diluted with achiral soldiers. The different outcomes of these chiral amplification phenomena are verified by modeling studies that reveal high mismatch penalties, which are ascribed to the high stereocenter loading of 12 methyl groups onto the monomers. Mixed-metal chiral amplification experiments between copper− and zinc−porphyrins show the same distinction in their mixing behavior, which is further supported by fluorescence measurements. The selective removal of chiral Zn−porphyrins from these mixed-metal systems is performed with the Lewis base quinuclidine that depolymerizes the Zn−porphyrins upon axial ligation. This extraction process proceeds at different time scales, depending on the mixed state: slow extraction kinetics for the mixed sergeant-and-soldiers and diluted-majority-rules systems and an instant extraction for the phase-separated majority-rules system. By simultaneously monitoring the supramolecular chirality during extraction, a chiral memory effect is observed for both mixed systems that show slow extraction kinetics. For the sergeant-and-soldiers system, the remaining supramolecular backbone contains achiral monomers only, which give rise to a long lasting chiral memory with slow, entropy-driven atropisomerization. Yet in case of the diluted-majority-rules system, the remaining backbone contains a mixture of achiral and chiral monomers in its unpreferred helicity; giving rise to a short chiral memory, in which the fast atropisomerization is enthalpy-driven due to the high mismatch penalty.

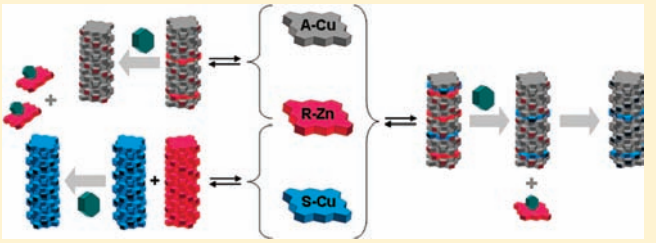

INTRODUCTION

The self-assembly of organic molecules is an interesting bottom-up approach to synthesize nanometer-sized devices.[1] Their functionality is afforded by multiple components that cooperate in these complex architectures, in which performance is highly dependent on the organization of these interacting moieties. The self-sorting of molecules provides valuable insights into this positional control.[2] In synthetic self-assembled systems, self-sorting behavior is often the result of the directionality of noncovalent interactions combined with steric constraints, as shown for rotaxane,[2] triangular,[3] and dendritic[4] structures. High-fidelity behavior could also be achieved by enantiomeric self-recognition,[5] in which the expression of chiral information leads to narcissistic self-sorting.[6] Interestingly, the helicity of supramolecular polymers can also be exploited to control the organization of molecules.

Helical supramolecular motifs are of great interest for the understanding of the origins of homochirality of biopolymers and the development of systems for chirotechnological applications.[7] Important aspects herein are embodied by self-assembled, helical, one-dimensional dye polymers that are the result of the supramolecular polymerization of the appropriate ditopic monomers. Recent studies reveal many similarities between macromolecules and supramolecular polymers, in which the latter class is more dynamic in nature.[9] Here, we utilize the dynamic properties of porphyrin-based aggregates to investigate if the self-sorting behavior can be controlled by the supramolecular helicity.

Different approaches have been exploited in order to control the helicity of racemic superstructures, for instance, by the employment of chiral auxiliaries,[10] enantioselective physical stimuli,[11] and chiral amplification.[12] In the latter approach, "sergeant-and-soldiers" experiments show that by mixing in a chiral "sergeant" with achiral "soldier" monomers, the handedness of helical aggregates containing predominantly achiral soldiers is biased by the chiral sergeant.[13] This results in a strong nonlinear chiroptical response, which is also observed in many majority-rules and diluted-majority-rules experiments. In these experiments, the helicity of an aggregate comprising two opposite enantiomers is dominated by the

Received: May 18, 2011
Published: June 29, 2011

Scheme 1. Chiral/Achiral Amide-Functionalized Tetraphenyl−Zinc/Copper−Porphyrins Used in This Study

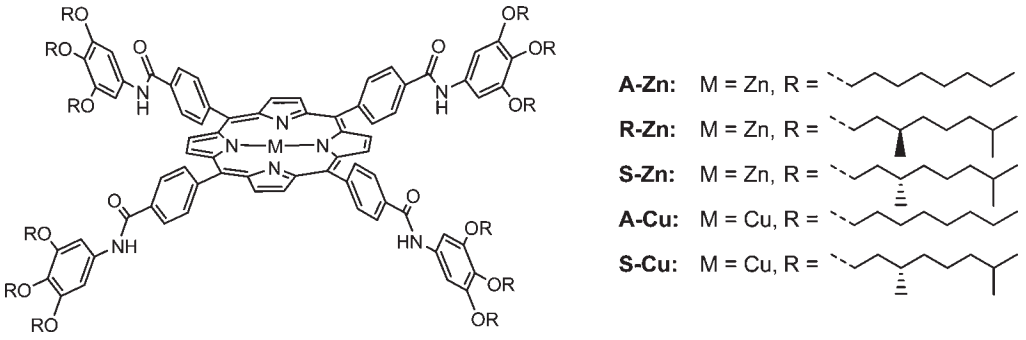

enantiomer in excess, and in case of the diluted-majority-rules, achiral soldiers are added to the system as well.[14] The nonlinear response of the optical activity in these chiral amplification experiments is caused by the subtle interplay of secondary interactions inside the supramolecular polymer. An enantiomeric imbalance introduced by one of the monomers is sufficient to transfer the chiral information to the supramolecular level, provided that both monomers are assembled in the same supramolecular polymer. For self-assembly of discotic molecules, the strength of these secondary interactions depends on the location,[15] number,[16] and type[17] of stereogenic centers in the chiral monomer. Over the years, our group has studied these effects in detail, for instance, by using different alkyl substituted, C_3-symmetrical benzene-1,3,5-tricarboxamides (BTAs). In chiral amplification studies, predictive models were developed and employed to deduce the interplay of secondary interactions in terms of two different energy penalties paid when different monomers are mixed in a stack.[18] Herein, the helix reversal penalty (HRP) describes the energy penalty of a helix reversal in the aggregate, whereas the mismatch penalty (MMP) is related to the incorporation of a chiral monomer in a helical aggregate of its unpreferred helicity.

Previously, we described a novel approach to obtain a chiral memory effect at the supramolecular level by a sergeant-and-soldiers experiment between **S-Zn** and **A-Cu** (Scheme 1) and the selective removal of **S-Zn** by the subsequent treatment with the Lewis base quinuclidine (QND).[19] In this contribution, we study chiral amplification with an expanded porphyrin library containing porphyrins with different stereochemistries in the periphery and different metal centers. We show that within this library highly distinctive mixed states can be achieved, which are rationalized by modeling studies, a fully mixed sergeant-and-soldiers system versus a narcissistically self-sorted majority-rules system. The selective removal of Zn−porphyrins by axial ligation with QND reveals a remarkable difference in their kinetics, which provides novel mechanistic insights into the mixing of porphyrins inside supramolecular polymers. For the first time, we use the diluted-majority-rules principle as a tool to mix opposite porphyrin enantiomers in a single stack by "dilution" of the system with achiral monomers. Thereby, we tune the removal rate of the chiral Zn−porphyrin from the system. For the purpose of constructing functional, multicomponent nanosized architectures, we envision that it is highly important to explore these chiral amplification phenomena since they could provide additional tools to place components at specified locations in the assembly. Additionally, these studies could also provide novel insights into the long lasting challenge of understanding the formation of racemates versus conglomerates in chiral drugs.[20]

DESIGN OF THE SYSTEM

The tetraphenyl porphyrins employed in this study have a symmetrical functionalization pattern with amide linkages to gallic moieties that contain achiral or branched chiral side chains in the periphery that bias the preferred helicity of their aggregates.[21] The porphyrins are provided with either copper or zinc ions in the center that allow fluorescence quenching studies and selective depolymerizations.[19] In methycyclohexane (MCH), all porphyrins show a hydrogen-bond-assisted and highly cooperative self-assembly process into one-dimensional H-type aggregates with a $\lambda_{max} \sim 390$ nm in the UV−vis spectrum that reveals the presence of extended cofacial aggregates, forming supramolecular polymers with a low free monomer concentration.[22] The chiral porphyrins (**R-Zn**, **S-Zn**, and **S-Cu**) show a strong CD effect in their Soret absorption, whereas achiral porphyrins (**A-Cu** and **A-Zn**) are CD-silent. In this study, all samples are prepared via chloroform injection of mixed monomer solutions in MCH. The low amount of chloroform (0.5 vol %) does not affect porphyrin aggregation or axial ligation of Zn−porphyrins with QND; hence, the injection technique affords thermodynamically stable aggregates in an efficient way.[19] For clarity, we refer to the term "coaggregation" when different porphyrin (co)monomers are mixed and share the same aggregate.

Previously, we reported on the sergeant-and-soldiers experiments of mixed-metal porphyrins in dilute MCH solutions, which revealed that chiral sergeant comonomers efficiently transfer their own chirality to achiral comonomers, yielding a helical aggregate with a single handedness.[19] Modeling of these data revealed high HRPs on the order of ~15 kJ mol^{-1}, which was attributed to the 4-fold hydrogen-bonding motif that causes a high energy barrier to overcome a helix reversal in the aggregate. In order to investigate the amplification of chirality in more detail, we perform majority-rules experiments as well, in which we can accurately determine MMPs. We start our studies with Zn−porphyrins where we describe the sergeant-and-soldiers experiments between **R**/**S-Zn** and **A-Zn**, after which we perform majority-rules experiments with both Zn-porphyrin enantiomers. In this paper, a special focus is maintained on the kinetic stability of the created metastable assemblies.

CHIRAL AMPLIFICATION OF ZN−PORPHYRINS AT ROOM TEMPERATURE

Figure 1A shows the CD spectra of **R-Zn**:**A-Zn** coaggregates at 1.0×10^{-6} M upon increasing the fraction of **R-Zn**. The shape of the CD spectrum remains unchanged upon enrichment of **R-Zn**, yet the CD intensity increases nonlinearly with the

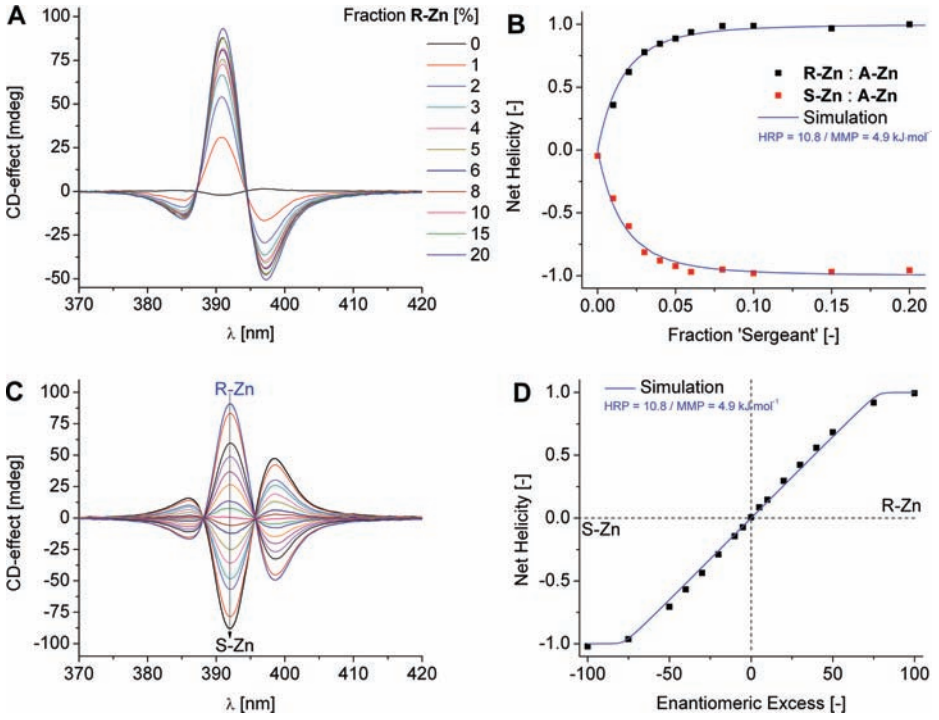

Figure 1. Sergeant-and-soldiers experiments of **R-Zn**/**S-Zn** and **A-Zn** at 1.0×10^{-6} M in MCH. (A) Full CD spectra of the **R-Zn**:**A-Zn** system recorded at 20 °C. (B) The net helicity as a function of the fraction of sergeants **R-Zn** and **S-Zn**. Majority-rules experiments of **R-Zn** and **S-Zn** at 1.0×10^{-6} M in MCH. (C) Full CD spectra recorded at 20 °C of mixtures of different ee as indicated by the arrow from pure **R-Zn** through ee = 0% (1:1 mixture) to pure **S-Zn**. (D) The net helicity as function of the ee. The blue lines in parts C and D show the overlay on both data sets at $\sigma = 1.41 \times 10^{-4}$ and $\omega = 0.135$ (10.8 and 4.9 kJ mol^{-1}) for the HRP and MMP, respectively.

composition, going from the CD-silent state of pure **A-Zn**[23] to a saturated, CD-active state at ~10% **R-Zn**. After conversion of the CD spectra to *g*-values at λ_{max} = 391 nm, we construct the net helicity versus the fraction sergeant (Figure 1B),[24] which shows mirror-image behavior of **R-Zn** with **A-Zn** and **S-Zn** with **A-Zn**. Both sergeant-and-soldiers experiments were simultaneously fitted with a modified model developed by van der Schoot.[18a] The least-squares fit on the experimental data in Figure 1B yields two dimensionless energy penalties, σ and ω, that represent the HRP and MMP, respectively, via $\sigma = \exp[-2\mathrm{HRP}/RT]$ and $\omega = \exp[-\mathrm{MMP}/RT]$. From the contour plot of the sum of squared residuals we can determine a HRP of ~14 kJ mol^{-1} quite accurately; however, an accurate determination of the MMP is difficult because of the wide spread in the plot for this penalty (Supporting Information Figure S3A).[21] The minimum of the contour plot of the sum of squared residuals is found at 16.6 and 0.2 kJ mol^{-1} for the HRP and MMP, respectively (Table 1). The high value for the HRP corresponds to the values we obtained in the sergeant-and-soldiers experiments for the mixed metal porphyrins described earlier,[19] which indicates that the nature of the center metal ion does not affect chiral amplification.

In order to obtain a more accurate determination of the MMP, majority-rules experiments are performed between **R-Zn** and **S-Zn**. Figure 1C shows the CD spectra of different enantiomeric mixtures at 1.0×10^{-6} M, going from pure **R-Zn** (ee = 100%) through **R-Zn**:**S-Zn** (1:1) (ee = 0%) to pure **S-Zn** (ee = −100%). The *g*-values at λ_{max} = 392 nm are used to construct the net helicity versus the ee (Figure 1D) and these data points show almost a linear trend. Apart from the homochiral samples, the linear relationship indicates that chiral amplification is absent,[17b]

Table 1. Overview of the Helix Reversal Penalty (HRP) and Mismatch Penalty (MMP) after Fitting the Different Chiral Amplification Experimental Data

experiment (figure)[a]	porphyrin mixture	HRP (kJ mol^{-1})[b]	MMP (kJ mol^{-1})[b]
S&S (1B)	**R/S-Zn**:**A-Zn**	16.6	0.2
MR (1D)	**R-Zn**:**S-Zn**	5.6	3.4
average (1B/D)	**R/A/S-Zn**	10.8	4.9
S&S (3A)	**S-Cu**:**A-Zn**	14.3	0.7
MR (3B)	**R-Zn**:**S-Cu**	15.4	11.2
DMR (4B)	**R-Zn**:**S-Cu**:**A-Cu**	9.5	2.6

[a] S&S, sergeant-and-soldiers experiment; MR, majority-rules experiment; DMR, diluted-majority-rules experiment. [b] The values for the HRP and MMP are obtained from the minimum of the contour plot of squared residuals. All contour plots are shown in the Supporting Information.

which is in contrast to what has been observed for BTAs[18a] and other supramolecular polymers.[14a,25] Here, saturated CD effects were observed at ee values far below 100%, indicative of a homochiral supramolecular system containing enantiomeric mixtures. The data are fitted with the majority-rules model,[18b] and from a similar contour plot a wide spread in the HRP is found, which makes an accurate estimation of this penalty difficult (Supporting Information Figure S5A). The MMP on the other hand could be accurately determined at ~4 kJ mol^{-1}, while the overall minimum of the contour plot is found at 5.6 and 3.4 kJ mol^{-1} for the HRP and MMP, respectively (Table 1).[21]

Similarly as shown for BTA's,[18a] we can obtain a single value for both energy penalties by considering the contour plots of

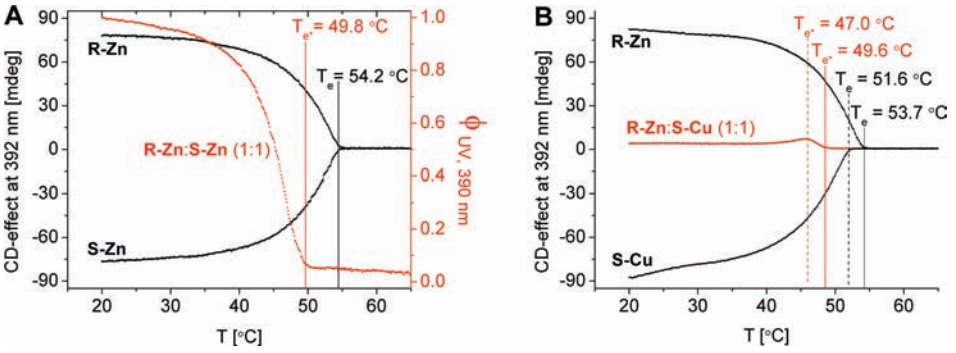

Figure 2. Cooling curves performed from the molecularly dissolved state at 65−20 °C at 60 °C/h in MCH at 1.0×10^{-6} M. (A) T_e analysis of the pure **R-Zn** and **S-Zn** enantiomers probed by CD at 392 nm (black, left axis) and the enantiomeric (1:1) mixture at ee = 0% probed by UV−vis at 390 nm (red, right axis). (B) Same experiment for the **R-Zn** and **S-Cu** system, all probed by CD at 392 nm.

both sergeant-and-soldiers and majority-rules experiments. This overall minimum is estimated at 10.8 and 4.9 kJ mol^{-1} for the HRP and MMP, respectively.[18] The simulation corresponding to these energy penalties overlays both chiral amplification data sets very well (Figure 1B/D, Table 1). These values are quite close to each other and reveal considerable energy penalties for both the HRP and MMP, indicating that it is highly unfavorable to both reverse a stack from one handedness to the other and to incorporate a chiral monomer in a stack of its opposite chirality. In these analyses, both energy penalties seem to be related to structural aspects of the monomer, with strong hydrogen bonding in the former[18a,19] and a high structural mismatch originating from 12 methyl groups in the latter. As a consequence, the likelihood that opposite enantiomers coaggregate would be significantly reduced when both energy penalties are high in this system, ultimately leading to narcissistic self-sorting into conglomerates comprising stacks with **R-Zn** or **S-Zn** only.

The extent of self-sorting herein is tested by the investigation of cooling curves performed on solutions of **R-Zn** and **S-Zn** at ee = 100%, 0%, and −100% at 1.0×10^{-6} M. Figure 2A shows the CD intensity at 392 nm upon cooling **R-Zn** (*ee* = 100%) and **S-Zn** (ee = −100%) from the molecularly dissolved state at 65−20 °C at 60 °C/h, which reveals nonsigmoidal cooling curves, indicating a highly cooperative self-assembly process.[22] The cooling curves for pure **R-Zn** and **S-Zn** are exact mirror images; both have a sharp transition at T_e = 54.2 °C and saturate at 79 and −78 mdeg, respectively. After converting the CD data to the dimensionless net helicity, both data sets are simultaneously fitted with a temperature-dependent nucleation−elongation model[26] from which we estimate an enthalpy release of 130 kJ mol^{-1}.[27] In the hypothesis of the formation of supramolecular conglomerates of **R-Zn** and **S-Zn**, no coaggregation of opposite enantiomers takes place, which implies an orthogonal self-assembly process upon cooling the mixture at ee = 0%. When cooling this 1:1 mixture of **R-Zn** and **S-Zn** at 1.0×10^{-6} M, no CD activity is observed, yet when probing the self-assembly process by UV−vis at λ_{max} = 390 nm, a similar, nonsigmoidal trend is observed with T_e = 49.8 °C (Figure 2A). By using the Van't Hoff relation, in which we correlate the total concentration to T_e at a fixed enthalpy value of 130 kJ mol^{-1}, we obtain a porphyrin concentration of 5×10^{-7} M that matches the T_e of the 1:1 mixture, exactly half the concentration of the enantiomerically pure systems.[21] This temperature analysis clearly indicates that both porphyrin enantiomers prefer the formation of their own stack with their own handedness, which is caused by the high structural mismatch. With this finding, we exceed an upper boundary for the mismatch penalty in chiral amplification, which is in contrast with the lower boundary we observed earlier for chiral deuterium-substituted BTAs that do not show a majority-rules effect due to the lack of helical bias induced by the isotope.[17a]

CHIRAL AMPLIFICATION OF MIXED-METAL ZN/CU−PORPHYRINS AT ROOM TEMPERATURE

In the present library, Cu−porphyrins are nonemissive, whereas Zn−porphyrins are highly emissive, albeit their fluorescence is partially quenched upon aggregation.[19] Still, the remaining aggregate fluorescence is more than sufficient for quenching studies with Cu−porphyrins that act as an energy trap when the two metal porphyrins are coaggregated, thereby monitoring the mixing of porphyrins with fluorescence. Quenching of the aggregate fluorescence was clearly observed in the previously described sergeant-and-soldiers between **S-Cu** and **A-Zn**, which showed that this process follows the amplification of chirality (Figure 3A). It can be observed that a fully homochiral system is obtained at 10% **S-Cu** and that ∼80% of the aggregate fluorescence is quenched.[28] Since no metal dependency was found for the chiral amplification behavior (vide supra, Table 1) and aggregate fluorescence can be used as a probe to investigate porphyrin coaggregation, we investigated the mixed-metal majority-rules experiment between **R-Zn** and **S-Cu**.

Analogously to the majority-rules experiments between **R-Zn** and **S-Zn**, we prepared samples in MCH by injection of monomer mixtures containing **R-Zn** and **S-Cu** at different ee in chloroform at 1.0×10^{-6} M. Since we prepared enantiomeric mixtures with the copper analogue of the **S-Zn** enantiomer, we observed slight differences in the UV−vis and CD spectra between **S-Cu** and **S-Zn**. As a result, **R-Zn** and **S-Cu** are not exactly mirror images and the ee = 0% sample does not reveal a completely CD-silent spectrum.[21] Still, when the CD intensity at 392 nm is converted to the *g*-value, the obtained net helicity versus ee shows a straight line (Figure 3B).

The linear relationship between the net helicity and ee is even more pronounced than for the homometal analogue of the majority-rules experiments, which is also expressed by the energy penalties obtained after fitting the data, 15.4 and 11.2 kJ mol^{-1} for the HRP and MMP, respectively (Table 1).[21] These chiral amplification data, in particular the high value for the MMP, clearly indicates that coaggregation between enantiomers is highly

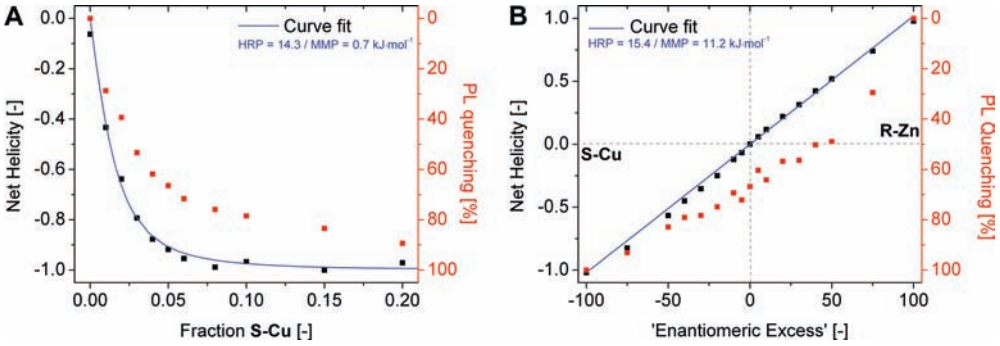

Figure 3. (A) Sergeant-and-soldiers experiments of **S-Cu**:**A-Zn** at 1.0×10^{-6} M in MCH at 20 °C. (B) Majority-rules experiments of **S-Cu**:**R-Zn** at 1.0×10^{-6} M in MCH at 20 °C. The net helicity (black, left axis) and fluorescence quenching (red, right axis) are plotted versus the fraction **S-Cu** (in A) and ee (in B), and the blue lines represent the model fits.

unfavorable, which can also be observed in the fluorescence response. Figure 3B shows only a weak deviation from linearity in the aggregate fluorescence, which indicates that quenching occurs only to a small extent. This is probably caused by (monomeric) Cu−porphyrin energy acceptors that approach the Zn−porphyrin stacks within the Föster distance. Quenching due to face-to-face stacking at the Zn−Cu−porphyrin heterojunction would significantly enhance fluorescence quenching, as we observe for the mixed-metal sergeant-and-soldiers experiments (Figure 3A). In this majority-rules experiment, only ∼20% quenching is observed at 10% **S-Cu** (ee = 80), which is significantly less than the ∼80% observed in the former experiment. This excludes a significant contribution to the quenching due to cofacial stacking. Additionally, the T_e analysis performed on this system indicates the formation of supramolecular conglomerates of **R-Zn** and **S-Cu** as well. The cooling curves show that **R-Zn** is more stable than **S-Cu**, as evidenced by their difference in T_e at 53.7 and 51.6 °C, respectively (Figure 2B).[29] Analogously to the T_e analysis for **R**/**S-Zn**, the enthalpy release for the pure enantiomers is obtained after fitting both cooling curves, and we probe the cooling of the **R-Zn**:**S-Cu** (1:1) mixture with CD at 392 nm.[21] When cooling this mixture at ee = 0% at 1.0×10^{-6} M, a positive CD response is observed at 49.6 °C; corresponding to the aggregation of **R-Zn**. Upon further cooling, the growth in optical activity ceases due to the aggregation of **S-Cu**, which starts at 47.0 °C. In their Van't Hoff analyses, both transition temperatures correspond to the predicted T_e's at 5×10^{-7} M for **R-Zn** and **S-Cu**, respectively. At lower temperatures, a nearly CD-silent state is obtained again due to the equal abundance of both aggregates with opposite helicity.

The chiral amplification experiments between mixed-metal porphyrins reveal the same features of porphyrin coaggregation as observed for the Zn−porphyrins; under the applied conditions, coaggregation of achiral and chiral porphyrins is feasible, unlike the coaggregation of opposite enantiomers. Considering the ease of helical induction of sergeant comonomers to the achiral backbone and the high energy barrier caused by the structural mismatch between the opposite enantiomers, it is highly interesting to investigate the possibility if the opposite enantiomers coaggregate in a stack that contains achiral soldiers as well. In order to investigate this possibility, we use the diluted-majority-rules principle,[18a,14c,14d] in which enantiomeric mixtures of **R-Zn** and **S-Cu** sergeants are "diluted" with **A-Cu** soldiers. The samples are prepared by chloroform injections of **R-Zn**/**S-Cu**/**A-Cu** monomer mixtures in MCH to a porphyrin concentration of 1.0×10^{-6} M. Figure 4A shows the sergeant-and-soldiers representation of this experiment with the *g*-value at λ_{max} = 390 nm versus the fraction sergeant, which represents enantiomeric mixtures of **R-Zn** and **S-Cu** at ee = 25, 50, and 75%.[21] The ee = 100% series herein represents the sergeant-and-soldiers of **R-Zn** and **A-Cu**, which is considered as the mirror image of **S-Zn** and **A-Cu** (ee = −100%).[30] Similar to the sergeant-and-soldiers principle, the diluted-majority-rules experiments show nonlinear amplification curves toward positive *g*-values originating from the majority of **R-Zn**, in which higher ee's result in higher *g*-values. The data at 100% sergeant represents the majority-rules experiment between **R-Zn** and **S-Cu**, which shows considerably lower *g*-values at this wavelength.[31] Related to the sergeant-and-soldiers experiment at ee = 100%, it can also be observed that a higher fraction of sergeant is necessary in order to obtain a fully homochiral system when the ee is lowered. From the amplification curves in Figure 4A it remains difficult to estimate whether coaggregation between both enantiomers takes place; however, when these diluted-majority-rules data are represented in a majority-rules plot, an obvious deviation from linearity is observed. This representation in Figure 4B shows the linear response between the net helicity and ee at 0% **A-Cu**, corresponding to the ("nondiluted") majority-rules experiment between **R-Zn** and **S-Cu** (Figure 3B). The net helicity for the highly diluted samples, e.g., at 80% **A-Cu**, is obtained from the *g*-values at 20% sergeant in Figure 4A. When these values at 25, 50, and 75% ee are normalized to the sergeant-and-soldiers at 100% ee, the obtained net helicity shows a positive deviation from linearity. This qualitative piece of evidence for chiral amplification is identical to the trend observed for most majority-rules systems, indicating that both enantiomers coaggregate in one stack.[14a,18a,25] We estimate from the fit on this deviation a HRP of 9.5 kJ mol^{-1} and a MMP of 2.6 kJ mol^{-1} (Table 1).[21] As expected, the HRP remains high since it refers to a similar H-type aggregate with strong hydrogen bonds that penalize a helix reversal. However, the MMP has considerably been reduced upon "dilution" with soldiers, which suggests that the structural mismatch between the opposite enantiomers is suppressed by the structural intrusion of achiral comonomers, hence resulting in a coaggregate containing **A-Cu**, **R-Zn**, and **S-Cu**.

■ SELECTIVE REMOVAL OF ZN−PORPHYRINS FROM CU/ZN-COAGGREGATES WITH QND

We reported on the selective depolymerization of Zn−porphyrins from coaggregated Cu/Zn systems,[19] which is performed

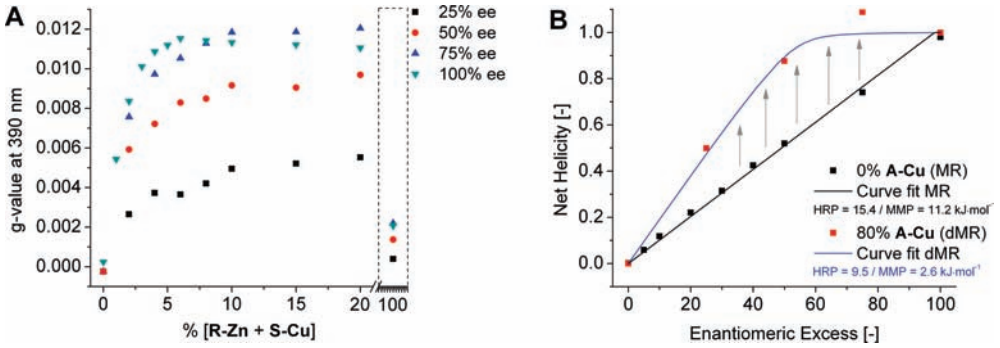

Figure 4. Diluted-majority-rules of **R-Zn** + **S-Cu** and **A-Cu** at 1.0×10^{-6} M in MCH at 20 °C. (A) *g*-Value at 390 nm versus the fraction [**R-Zn** + **S-Cu**] sergeant for ee values of 25, 50, and 75%. The 100% ee data set equals the sergeant-and-soldiers experiment of **R-Zn** and **A-Cu**, which is considered as the mirror image of **S-Zn** and **A-Cu**, and the boxed data points at 100% sergeant equal the majority-rules experiment of **R-Zn** and **S-Cu** at 390 nm (Supporting Information Figure S8D). (B) The same experiment represented as the net helicity versus ee with the corresponding fits on the nondiluted and 80% diluted state.

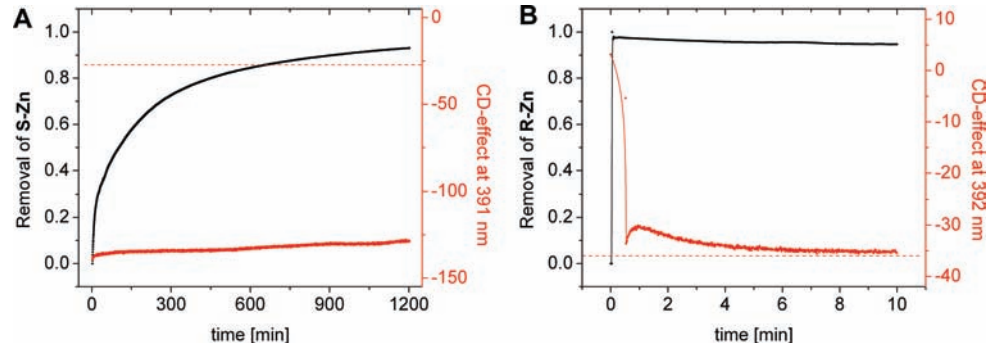

Figure 5. Kinetic profile of the extraction of **S-Zn** of **S-Zn**:**A-Cu** (1:9) coaggregates at a porphyrin concentration of 1.0×10^{-6} M and a QND concentration of 1.0×10^{-2} M in MCH at 20 °C; the conversion of the **S-Zn**:QND as probed by UV−vis at $\lambda_{max} \sim 431$ nm (black axis, left) and CD (red axis, right) versus time (A). Similar profile for the extraction of **R-Zn** from the **R-Zn**:**S-Cu** (1:1) system under identical conditions (B).

with quinuclidine (QND) that caps free Zn−monomers that are involved in the aggregate−monomer equilibrium.[22] Upon Zn−QND complexation, one porphyrin plane gets sterically blocked, which inhibits the formation of hydrogen bonds between adjacent porphyrins. By this scavenging process, free Zn−monomers are selectively extracted and removed from the self-assembling system. The mixed-metal sergeant-and-soldiers experiments between chiral and achiral comonomers reveal coaggregation with amplification of chirality, whereas no amplification of chirality is observed in the mixed-metal majority-rules reaction as a result of narcissistic self-sorting. By the combination of both chiral amplification phenomena, coaggregation of enantiomers becomes feasible when the stacks are "diluted" with achiral comonomers. By proper choice of center metal and side chain identity, we can selectively extract Zn−porphyrins from these mixed-metal sergeant-and-soldiers[19] and (diluted-)majority-rules systems. By simultaneously monitoring the supramolecular chirality and extraction kinetics, we can study the observed differences in these porphyrin coaggregates in more detail. In our kinetic investigations on mixed-metal sergeant-and-soldiers and (diluted-)majority-rules systems, we perform the Zn−porphyrin extractions on a total porphyrin concentration of 1.0×10^{-6} M and we use a 10 000 times excess of QND. Under these conditions, we fully remove all Zn−porphyrins from the coaggregates and ensure the exclusive formation of monomeric complexes that absorb at $\lambda_{max} = 431$ nm; hence, by time-dependent monitoring of this wavelength we can probe this removal process.

Figure 5A shows the kinetic plot of the removal of **S-Zn** from **S-Zn**:**A-Cu** (1:9) coaggregates, in which the receptive sergeant is present at a concentration of 1.0×10^{-7} M. This time-dependent UV−vis measurement at 431 nm reveals extremely slow extraction kinetics; only after ∼15 h all Zn−porphyrins are converted to **S-Zn**:QND complexes, as evidenced by the UV−vis absorption. Earlier, we attributed this slow kinetics to the low concentration of receptive **S-Zn** comonomers and the slow exchange between monomers and aggregates.[19] Upon the extraction of sergeant, the preferred helicity of the remaining **A-Cu** backbone remains present and the full optical activity after ∼15 h indicates a chiral memory effect.

In the narcissistically self-sorted majority-rules system with **R-Zn** and **S-Cu**, we selected the sample at ee = 0%, which is CD-silent due to equal abundance of **R-Zn** stacks and **S-Cu** stacks in solution. When we add QND to this system with 5.0×10^{-7} M receptive **R-Zn**, we observe *instant* depolymerization; ∼1 min after the addition of 1.0×10^{-2} M QND the absorption band of the **R-Zn**:QND band at 431 nm has fully developed (Figure 5B). Similar kinetic behavior has been observed with pyridine titration to **S-Zn** homoaggregates, indicating rapid depolymerization of **R-Zn** stacks.[22] Upon the removal of **R-Zn**, it can be observed that the CD response follows UV; going from a CD-silent state at

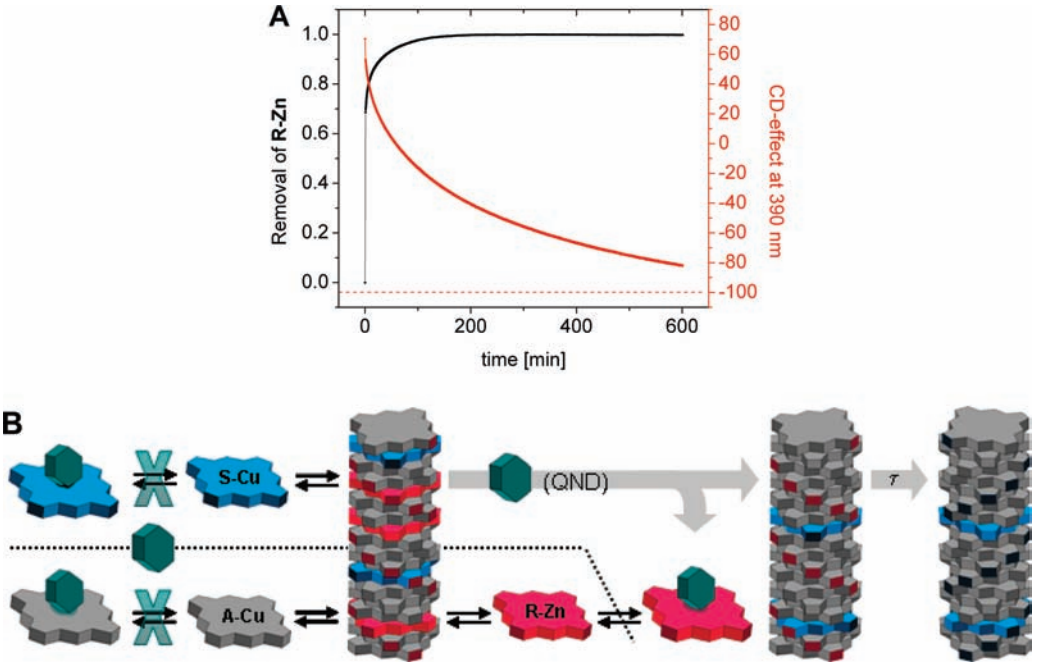

Figure 6. Kinetic profile of the extraction of **R-Zn** from the **R-Zn**:**S-Cu**:**A-Cu** (12.5:7.5:80) system at a porphyrin concentration of 1.0×10^{-6} M and a QND concentration of 1.0×10^{-2} M in MCH at 20 °C; the conversion of the **R-Zn**:QND as probed by UV−vis at $\lambda_{max} \sim 431$ nm (black axis, left) and CD (red axis, right) versus time (A). Schematic depiction of the selective removal of **R-Zn** from the diluted-majority-rules system with a reversal of the supramolecular chirality (B).

ee = 0% to a CD active state originating from ee = −100% from **S-Cu** stacks at 5.0×10^{-7} M. The simultaneous response of CD and UV reveals the absence of a chiral memory effect, and it supports the self-sorted character of the **R-Zn**:**S-Cu** system.

Under the assumption that the dynamics for monomer−aggregate exchange does not strongly depend on the metal/side chain of the porphyrin, the remarkable difference in extraction kinetics between the coaggregated **S-Zn**:**A-Cu** (1:9) and the narcissistically self-sorted **R-Zn**:**S-Cu** (1:1) system can be rationalized by a shielding effect that occurs when Zn−porphyrins are coaggregated with Cu−porphyrins. This hypothesis can be explained by the exposure of porphyrin monomers when they detach from the end from the stack in order to preserve the dynamic equilibrium between monomers and aggregates. In the case of efficient coaggregation, the Zn−porphyrins are homogeneously distributed over the mixed stack, and the monomers that keep the whole coaggregate in the equilibrated state comprise Zn− as well as Cu−porphyrins. As a result, Zn−monomer exposure occurs to a considerably lower extent than when the Zn−porphyrins form their own homoaggregate, in which only Zn−monomers are involved in the equilibrium. In the latter, each monomer exposure event leads to monomer scavenging, which causes a shift in the equilibrium, hence leading to depolymerization. In this way, Cu−porphyrins "protect" the Zn−porphyrins by consistent participation in the dynamic equilibrium. We therefore postulate that Zn−monomers are removed more slowly when they are coaggregated with Cu−monomers.

The chiral amplification experiments on the diluted-majority-rules system indicate that coaggregation of enantiomers is enabled upon "dilution" with soldier comonomers that encounter a lower structural mismatch (Figure 4B). This behavior *between* sergeant-and-soldiers and majority-rules is also observed in its extraction process with QND, as we show for the **R-Zn**:**S-Cu**:**A-Cu** (12.5:7.5:80, ee = 25% at 20% sergeant) coaggregate. At a concentration of 1.25×10^{-7} M, the **R-Zn** sergeant dominates the helical sense of this coaggregate, which shows a positive CD signal at 392 nm (Figure 4A). Upon the removal of **R-Zn** from this diluted-majority-rules system we observe slow extraction kinetics; after ∼200 min all Zn−porphyrins are converted to **R-Zn**:QND complexes (Figure 6A). The extraction kinetics is in line with the sergeant-and-soldiers experiment, yet in this coaggregate, **S-Cu** and **A-Cu** comonomers are predominantly involved in the dynamic equilibrium, thereby protecting **R-Zn** from axial ligation (Figure 6B). Remarkably, when we consider the chirality of the supramolecular backbone during extraction, we observe an optical response *between* sergeant-and-soldiers and majority-rules systems. Upon **R-Zn** removal, a direct response in CD is observed; however, the CD response does not follow the absorbance of **R-Zn**:QND. When all **R-Zn** comonomers are removed at ∼200 min, the chirality is halfway the transition from a positive to a negative helical sense, which originates from the remaining **S-Cu**:**A-Cu** (7.5:80) coaggregate. The observed chiral memory effect fully disappears after 1 day, which is in contrast with chiral memory effect of the remaining **A-Cu** backbone in the **S-Zn**:**A-Cu** (1:9) coaggregate that lasts over months.[19]

The difference between these memory effects is obviously related to frustration caused by **S-Cu**, which is initially incorporated in a stack of the wrong handedness. Therefore, the initial **R-Zn**:**S-Cu**:**A-Cu** (12.5:7.5:80) coaggregates are higher in energy than the final state, where **R-Zn** has been removed, which causes a rapid, enthalpy-driven atropisomerization. Since **A-Cu** lacks the preference for any helical direction, this energy difference caused by initial structural frustration is absent; as a result, the atropisomerization is entropy driven and slow due to the conformational inertness of the **A-Cu** backbone.

CONCLUSION

The coaggregation behavior of porphyrins with different metals and side chains was investigated by chiral amplification. Efficient coaggregation was observed between achiral and chiral porphyrins, as evidenced by a strong sergeant-and-soldiers effect. On the other hand, no chiral amplification was observed in the majority-rules experiment. The distinctive behavior in chiral amplification was quantified by modeling studies that revealed a combination of high helix reversal and high mismatch penalties, on the order of 10 and 5 kJ mol^{-1}, respectively. The high mismatch penalty explains the absence of a majority-rules effect; the conformational mismatch between the opposite enantiomers does not allow coaggregation. Rather, narcissistic self-sorting of the enantiomers is observed, as shown by cooling studies.

The chiral amplification behavior does not depend on the metal center inside the porphyrin. Mixed-metal sergeants-and-soldiers and majority-rules studies also showed highly distinctive mixing, which was also supported with the fluorescence quenching between Zn− and Cu−porphyrins. The limits of coaggregation were further explored with diluted-majority-rules measurements, which showed a chiral amplification effect, indicating that both enantiomers coaggregate when the stacks contain achiral comonomers as well. Compared to the mixed-metal majority-rules experiment, lower mismatch penalties were estimated after fitting the diluted-majority-rules experiment.

Besides chirality and fluorescence, we performed kinetic experiments in order to investigate the coaggregation behavior in more detail. Studies on the selective extraction of Zn−porphyrins from mixed-metal sergeant-and-soldiers and (diluted-) majority-rules systems showed remarkable differences in their rate of chiral Zn−porphyrin removal. For the coaggregated systems, slow extraction kinetics was found, whereas an instant Zn−porphyrin removal was found for the narcissistically self-sorted system. A mechanistic explanation for this rate difference relies on the susceptibility of monomers that are in equilibrium with the (co-)aggregates; Cu−porphyrins "protect" Zn−porphyrins by their monomer exposure in order to retain the equilibrium of the coaggregate.

The chiral response upon the removal of chiral Zn−porphyrins reveals a chiral memory effect for the coaggregated systems due to the kinetic inertness of the achiral backbone. For the sergeant-and-soldiers system, a long lasting memory is found, whereas a short memory was found for the diluted-majority-rules system. The memory difference is caused by the opposite Cu−enantiomer that remains coaggregated with the achiral backbone in the latter, which frustrates the helical imprint and causes an energy difference; hence, a fast, enthalpy-driven atropisomerization is observed. Yet for the sergeant-and-soldiers system, this energy difference before and after selective extraction is not present, which results in a slow, entropy-driven atropisomerization.

As evidenced by the chiral amplification phenomena, we achieved highly distinctive mixed states within the porphyrin assemblies by only subtle peripherical changes in the monomer. Within the same library, we can use the diluted-majority-rules principle as a tool to control the extent of mixing. For the purpose of constructing functional, multicomponent nanoarchitectures, we envision that it is highly interesting to explore these chiral amplification phenomena, since they could provide additional tools to control stoichiometry and place the components at specified locations in the assembly. On the other hand, this type of stereochemical control may also provide mechanistic insights into dynamic mixing.

ASSOCIATED CONTENT

Supporting Information. The synthesis of the **R-Zn** and UV−vis/CD/PL spectra of all chiral amplification experiments with corresponding contour plots and calculations on cooling curves. This material is available free of charge via the Internet at http://pubs.acs.org.

AUTHOR INFORMATION

Corresponding Author
A.P.H.J.Schenning@tue.nl; E.W.Meijer@tue.nl

ACKNOWLEDGMENT

This work was supported by the Council of Chemical Sciences of The Netherlands Organization for Scientific Research (CW-NWO). We thank Marko Nieuwenhuizen and Peter Korevaar for stimulating discussions, and Dr. Martin Wolffs and Juliën van Velthoven for early contributions to the project.

REFERENCES

(1) (a) Kay, E. R.; Leigh, D. A.; Zerbetto, F. *Angew. Chem., Int. Ed.* **2007**, *46*, 72–191. (b) Schenning, A.; Meijer, E. W. *Chem. Commun.* **2005**, 3245–3258.

(2) (a) Jiang, W.; Schalley, C. A. *Proc. Natl. Acad. Sci. U. S. A.* **2009**, *106*, 10425–10429. (b) Jiang, W.; Winkler, H. D. F.; Schalley, C. A. *J. Am. Chem. Soc.* **2008**, *130*, 13852–13853.

(3) (a) Schmittel, M.; Mahata, K. *Chem. Commun.* **2010**, *46*, 4163–4165. (b) Mahata, K.; Saha, M. L.; Schmittel, M. *J. Am. Chem. Soc.* **2010**, *132*, 15933–15935.

(4) Corbin, P. S.; Lawless, L. J.; Li, Z. T.; Ma, Y. G.; Witmer, M. J.; Zimmerman, S. C. *Proc. Natl. Acad. Sci. U. S. A.* **2002**, *99*, 5099–5104.

(5) (a) Hutin, M.; Cramer, C. J.; Gagliardi, L.; Shahi, A. R. M.; Bernardinelli, G.; Cerny, R.; Nitschke, J. R. *J. Am. Chem. Soc.* **2007**, *129*, 8774–8780. (b) Shi, X. D.; Fettinger, J. C.; Davis, J. T. *J. Am. Chem. Soc.* **2001**, *123*, 6738–6739.

(6) (a) Taylor, P. N.; Anderson, H. L. *J. Am. Chem. Soc.* **1999**, *121*, 11538–11545. (b) Wu, A. X.; Isaacs, L. *J. Am. Chem. Soc.* **2003**, *125*, 4831–4835.

(7) (a) Mateos-Timoneda, M. A.; Crego-Calama, M.; Reinhoudt, D. N. *Chem. Soc. Rev.* **2004**, *33*, 363–372. (b) Okamoto, Y.; Nakano, T. *Chem. Rev.* **1994**, *94*, 349–372. (c) Verbiest, T.; Van Elshocht, S.; Kauranen, M.; Hellemans, L.; Snauwaert, J.; Nuckolls, C.; Katz, T. J.; Persoons, A. *Science* **1998**, *282*, 913–915. (d) Maeda, K.; Yashima, E. *Top. Curr. Chem.* **2006**, *265*, 47–88.

(8) Lee, C. C.; Grenier, C.; Meijer, E. W.; Schenning, A. *Chem. Soc. Rev.* **2009**, *38*, 671–683.

(9) Yashima, E.; Maeda, K.; Nishimura, T. *Chem.—Eur. J.* **2004**, *10*, 42–51.

(10) (a) George, S. J.; Tomovic, Z.; Smulders, M. M. J.; de Greef, T. F. A.; Leclere, P.; Meijer, E. W.; Schenning, A. *Angew. Chem., Int. Ed.* **2007**, *46*, 8206–8211. (b) Fenniri, H.; Deng, B. L.; Ribbe, A. E. *J. Am. Chem. Soc.* **2002**, *124*, 11064–11072. (c) Ishi-i, T.; Crego-Calama, M.; Timmerman, P.; Reinhoudt, D. N.; Shinkai, S. *Angew. Chem., Int. Ed.* **2002**, *41*, 1924–1929. (d) Oda, R.; Huc, I.; Schmutz, M.; Candau, S. J.; MacKintosh, F. C. *Nature* **1999**, *399*, 566–569. (e) El-Hachemi, Z.; Mancini, G.; Ribo, J. M.; Sorrenti, A. *J. Am. Chem. Soc.* **2008**, *130*, 15176–15184. (f) Jiang, S. G.; Zhang, L.; Liu, M. H. *Chem. Commun.* **2009**, 6252–6254. (g) Rosaria, L.; D'Urso, A.; Mammana, A.; Purrello, R. *Chirality* **2008**, *20*, 411–419. (h) Toyofuku, K.; Alam,

M. A.; Tsuda, A.; Fujita, N.; Sakamoto, S.; Yamaguchi, K.; Aida, T. *Angew. Chem., Int. Ed.* **2007**, *46*, 6476–6480.

(11) (a) Janssen, P. G. A.; Ruiz-Carretero, A.; Gonzalez-Rodriguez, D.; Meijer, E. W.; Schenning, A. *Angew. Chem., Int. Ed.* **2009**, *48*, 8103–8106. (b) El-Hachemi, Z.; Arteaga, O.; Canillas, A.; Crusats, J.; Escudero, C.; Kuroda, R.; Harada, T.; Rosa, M.; Ribo, J. M. *Chem.—Eur. J.* **2008**, *14*, 6438–6443. (c) Tejedor, R. M.; Oriol, L.; Serrano, J. L.; Urena, F. P.; Gonzalez, J. J. L. *Adv. Funct. Mater.* **2007**, *17*, 3486–3492.

(12) Palmans, A. R. A.; Meijer, E. W. *Angew. Chem., Int. Ed.* **2007**, *46*, 8948–8968.

(13) (a) Palmans, A. R. A.; Vekemans, J.; Havinga, E. E.; Meijer, E. W. *Angew. Chem., Int. Ed.* **1997**, *36*, 2648–2651. (b) Green, M. M.; Reidy, M. P.; Johnson, R. J.; Darling, G.; Oleary, D. J.; Willson, G. *J. Am. Chem. Soc.* **1989**, *111*, 6452–6454.

(14) (a) van Gestel, J.; Palmans, A. R. A.; Titulaer, B.; Vekemans, J.; Meijer, E. W. *J. Am. Chem. Soc.* **2005**, *127*, 5490–5494. (b) Green, M. M.; Garetz, B. A.; Munoz, B.; Chang, H. P.; Hoke, S.; Cooks, R. G. *J. Am. Chem. Soc.* **1995**, *117*, 4181–4182. (c) Wilson, A. J.; van Gestel, J.; Sijbesma, R. P.; Meijer, E. W. *Chem. Commun.* **2006**, 4404–4406. (d) Selinger, J. V.; Selinger, R. L. B. *Macromolecules* **1998**, *31*, 2488–2492.

(15) Stals, P. J. M.; Smulders, M. M. J.; Martin-Rapun, R.; Palmans, A. R. A.; Meijer, E. W. *Chem.—Eur. J.* **2009**, *15*, 2071–2080.

(16) (a) Iavicoli, P.; Xu, H.; Feldborg, L. N.; Linares, M.; Paradinas, M.; Stafstrom, S.; Ocal, C.; Nieto-Ortega, B. L.; Casado, J.; Navarrete, J. T. L.; Lazzaroni, R.; De Feyter, S.; Amabilino, D. B. *J. Am. Chem. Soc.* **2010**, *132*, 9350–9362. (b) Smulders, M. M. J.; Stals, P. J. M.; Mes, T.; Paffen, T. F. E.; Schenning, A. P. H. J.; Palmans, A. R. A.; Meijer, E. W. *J. Am. Chem. Soc.* **2010**, *132*, 620–6.

(17) (a) Cantekin, S.; Balkenende, D. W. R.; Smulders, M. M. J.; Palmans, A. R. A.; Meijer, E. W. *Nature Chem.* **2011**, *3*, 42–46. (b) Veld, M. A. J.; Haveman, D.; Palmans, A. R. A.; Meijer, E. W. *Soft Matter* **2011**, *7*, 524–531.

(18) (a) Smulders, M. M. J.; Filot, I. A. W.; Leenders, J. M. A.; van der Schoot, P.; Palmans, A. R. A.; Schenning, A. P. H. J.; Meijer, E. W. *J. Am. Chem. Soc.* **2010**, *132*, 611–619. (b) van Gestel, J. *Macromolecules* **2004**, *37*, 3894–3898.

(19) Helmich, F.; Lee, C. C.; Schenning, A. P. H. J.; Meijer, E. W. *J. Am. Chem. Soc.* **2010**, *132*, 16753–16755.

(20) Wang, Y. L.; Chen, A. M. *Org. Process Res. Dev.* **2008**, *12*, 282–290.

(21) See Supporting Information

(22) Helmich, F.; Lee, C. C.; Nieuwenhuizen, M. M. L.; Gielen, J. C.; Christianen, P. C. M.; Larsen, A.; Fytas, G.; Leclere, P.; Schenning, A.; Meijer, E. W. *Angew. Chem., Int. Ed.* **2010**, *49*, 3939–3942.

(23) The CD spectrum of **A-Zn** shows a small CD effect, which is most likely due to enantiomeric impurities.

(24) The net helicity is obtained from dividing the *g*-value at a certain composition by the maximum *g*-value at λ_{max}. The *g*-value is the anisotropy factor, which is calculated via $g = \Delta\varepsilon/\varepsilon = \text{CD-effect}\,[\text{mdeg}]/(32\,980 \times \text{OD})$.

(25) (a) Jin, W.; Fukushima, T.; Niki, M.; Kosaka, A.; Ishii, N.; Aida, T. *Proc. Natl. Acad. Sci. U. S. A.* **2005**, *102*, 10801–10806. (b) Lohr, A.; Wurthner, F. *Angew. Chem., Int. Ed.* **2008**, *47*, 1232–1236.

(26) Smulders, M. M. J.; Schenning, A. P. H. J.; Meijer, E. W. *J. Am. Chem. Soc.* **2008**, *130*, 606–610.

(27) The enthalpy value differs slightly from the one we published earlier,[22] which is most likely related to monomer purity and the preparation method with chloroform.

(28) The percentage of quenching is determined by the difference in luminescence between pure **A-Zn** (100%) and pure **S-Cu** (0%) at the emission maximum at λ_{max} = 604 nm.[21]

(29) The difference in T_e for **R-Zn** in Figure 2A,B is caused by a concentration effect, as evidenced by a lower absorption for the latter at λ_{max}.

(30) Considering the mirror-image behavior in chiral amplification of **R**/**S-Zn** with **A-Zn** (Figure 1B), we assume the same behavior for the amplification of **A-Cu**.

(31) The CD spectra of amplified, achiral porphyrins observed in sergeant-and-soldiers experiments have a different shape than the CD spectra of intrinsically chiral aggregates.[21]